

The effects of boric acid on crystal structure, nano-/microstructure and photoluminescence characteristics of rare earth-doped Y_2O_3/YBO_3 composite compounds

Seyed Mahdi Rafiaei¹  · Abbas Bahrami²

Received: 20 September 2017 / Accepted: 30 October 2017 / Published online: 7 November 2017
© The Author(s) 2017. This article is an open access publication

Abstract In this investigation, $(Y_{0.96}Eu_{0.04})_2O_3$ phosphor nanoparticles with an average size of 85 nm were synthesized through a facile solid-state method. It was found that small magnitudes of H_3BO_3 improve both growth and crystallinity of nanoparticles, significantly. Consuming specific amounts of boric acid not only results in dramatic changes in crystal structure, from cubic to hexagonal, but also influences size and morphology of particles. Noteworthy, further increase in the additive suppresses the crystal growth procedure. The luminescent properties of

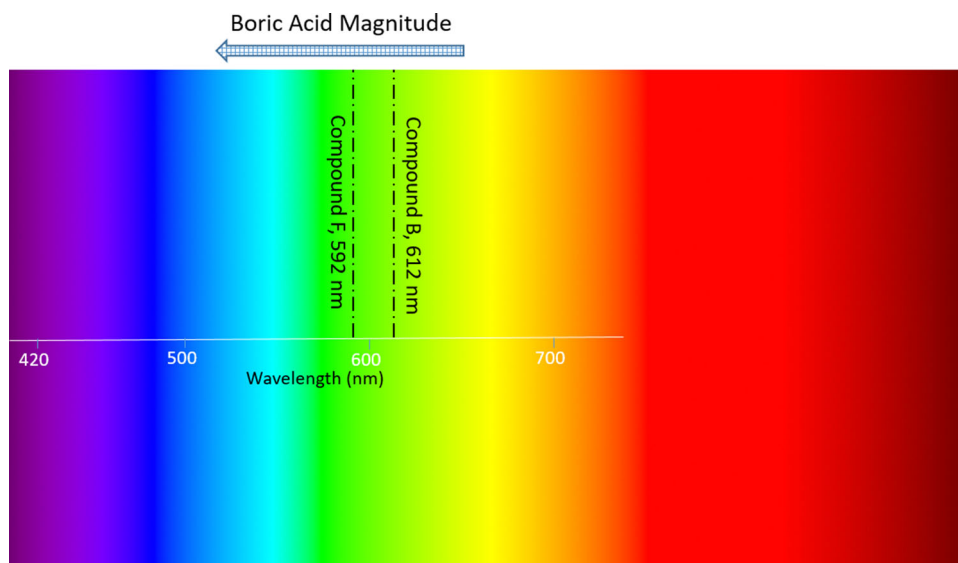
the synthesized phosphors were investigated by PL analyzer. It was found that the change in crystal structure leads to the huge differences in the wavelength and the photoluminescence characteristics. The main emission bands of Y_2O_3 - and YBO_3 -based compounds are attributed to 5D_0 - 7F_2 electric dipole and 5D_0 - 7F_1 magnetic dipole transitions, respectively. In other words, it was concluded that sufficient quantities of H_3BO_3 cause a noticeable decrease in the main emission wavelength from 612 to 592 nm.

✉ Seyed Mahdi Rafiaei
rafiaei@gut.ac.ir

¹ Department of Materials Science and Engineering,
Golpayegan University of Technology, Golpayegan, Iran

² Department of Materials Engineering, Isfahan University of
Technology, Isfahan 84156-83111, Iran

Graphical Abstract



Keywords Boric acid · Nanoparticles · Phosphors · Luminescence · Emission

Introduction

Recently, phosphor compounds have been a subject of interest and controversy, and among them Y_2O_3 has an exceptional status. Yttrium oxide with a space group Ia3 (No. 206) and cubic crystal structure, density of about 5.01 g/cm^3 , refractive index more than 1.9, a wide band gap of 5.8 eV and melting point over $2400 \text{ }^\circ\text{C}$ has been known as one of the most efficient phosphors in the area of optic materials. Yttria is widely used in many applications in various fields such as white LEDs [1], photovoltaic cells, up-conversion phosphors [2], lighting, sensors, and transparent ceramics [3], due to its excellent chemical stability. In addition, the literature surveys show that Yttria has been widely employed as host lattice for many lanthanide dopants like Eu and Tb ions [4]. The rare earth ions are characterized by semi-filled 4f shells. In these ions, 4f orbitals are located in inner layers shielded by filled 5s and 5p orbitals. Correspondingly, referring to this shielding phenomenon, the effect of host lattice on optical transitions through 4f configuration is not very significant. Also, in configurational coordinate diagram (CCD) the levels of energy can be considered as parallel graph ($\Delta R = 0$). Among the lanthanide ions, Eu^{3+} with ${}^5D_0 \rightarrow {}^7F_2$ transition has been used extensively as a source of red light at an approximate wavelength of 618 nm [5].

The studies about Y_2O_3 reveal that different methods have been used to synthesize it, e.g., hydrothermal [6, 7], sol-gel [8], spray pyrolysis [9], combustion [10, 11], co-

precipitation [12], micro-emulsion microwave [13] and electrospinning [14]. From the mentioned techniques, many researchers prefer to prepare phosphor materials through relatively simple solid-state method. But it should be noticed that this method has its own disadvantages, like improper crystallinity and calcinations at high temperatures. Therefore, to overcome these weak points many flux materials are used through solid-state process [15]. As a matter of fact, the melting point of flux compounds is less than the temperature of solid-state reaction, resulting in simplifying the reaction at lower temperatures. H_3BO_3 with the melting point of $171 \text{ }^\circ\text{C}$ is one of the most prominent flux materials, employed for synthesizing Y_2O_3/Gd_2O_3 compounds [16].

Motivated by this background, the effect of different amounts of boric acid on microstructure, crystal structure and optical properties of synthesized phosphors was studied. Also, the influences of the magnitude of this additive on the properties of $(Y_{0.96}Eu_{0.04})_2O_3$ phosphors were investigated. In this work, XRD, FESEM and PL analyses were employed to evaluate the crystal structure, size and morphology of synthesized powders and also their photoluminescence characteristics.

Experimental

Preparation

To synthesize $(Y_{0.96}Eu_{0.04})_2O_3$ phosphor, analytical grades of yttrium acetate $Y(CH_3COO)_3 \cdot xH_2O$, europium oxide (Eu_2O_3) were purchased from Aldrich Company with the highest purity (99.99%), used without any purification. In a



typical procedure, 1 g of yttrium acetate together with 0.026 g of europium oxide was ground in an alumina crucible. Then, this mixture was calcined at 1100 °C for 2 h in air, using a tube furnace. In this research, the considered productions nominated as A, B, C, D, E, F, G, H and I compounds were synthesized through using different amounts of H_3BO_3 , added to the explained initial materials (see Table 1). The produced materials are hereafter. Accordingly, R shows the ratio of used boric acid to the required stoichiometric boric acid.

Characterization

The crystal structures of synthesized $\text{Y}_2\text{O}_3/\text{YBO}_3:\text{Eu}^{3+}$ phosphors were examined by X-ray diffraction (XRD, Rigaku, Japan) with $\text{CuK}\alpha$ radiation ($\lambda = 1.54 \text{ \AA}$). To study the microstructure and size of these phosphors, field emission scanning electron microscope (FESEM, Hitachi SU70, Japan) and also Brunauer–Emmett–Teller (BET, Sensiran, Toseye Heshgarsazan Asia, Iran) were employed. In addition, the optical characteristics of synthesized phosphors were investigated through use of photoluminescence (PL, Horiba Jobin–Yvon Fluorolog-3, Japan) analyzer.

Results and discussion

XRD analysis

Figure 1a shows the XRD spectra of $\text{Y}_2\text{O}_3/\text{YBO}_3:\text{Eu}^{3+}$ phosphors (A–H compounds). The spectra of A–D compounds show that the main peaks of diffraction are attributed to (211), (222), (400), (440) and (622) crystallographic planes indicating that the synthesized phosphor has cubic structure (JCPDS No. 41-1105). For the sample A, the crystallite size of 45.6 nm was calculated employing the Scherrer formula, $D = 0.9\lambda/\beta\cos\theta$. In this

Table 1 Name of different compounds due to magnitude of added H_3BO_3

Compound	Compound	R
A	$\text{Y}_2\text{O}_3:\text{Eu}^{3+}$	0
B	$\text{YBO}_3:\text{Eu}^{3+}$	0.02
C	$\text{YBO}_3:\text{Eu}^{3+}$	0.05
D	$\text{YBO}_3:\text{Eu}^{3+}$	0.15
E	$\text{YBO}_3:\text{Eu}^{3+}$	0.25
F	$\text{YBO}_3:\text{Eu}^{3+}$	0.5
G	$\text{YBO}_3:\text{Eu}^{3+}$	1
H	$\text{YBO}_3:\text{Eu}^{3+}$	2
I	$\text{YBO}_3:\text{Eu}^{3+}$	4

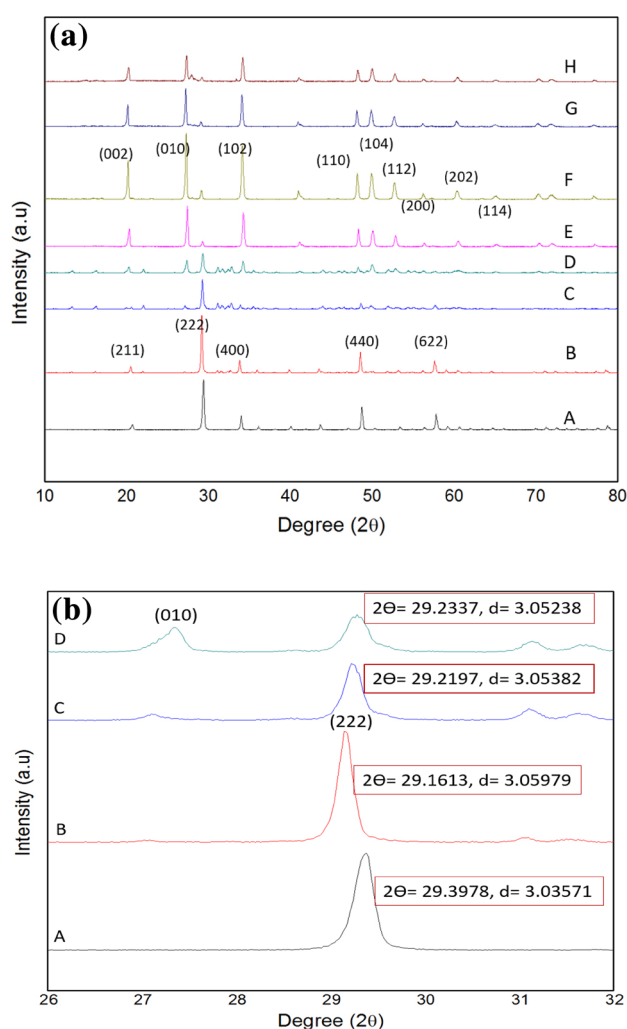


Fig. 1 XRD spectra of $\text{Y}_2\text{O}_3/\text{YBO}_3:\text{Eu}^{3+}$ phosphors: **a** A–H and **b** A–D luminescent compounds

equation, D is the average grain size, λ is the wavelength of X-ray (0.154 nm), and β and θ are the full-width at half-maximum and diffraction angle of an observed peak, respectively. Accordingly, it is obvious that whenever R varies from 0 to 0.25, the structure of synthesized compound is very similar to that of Y_2O_3 , with a cubic crystal structure. Among the mentioned crystallographic planes, the intensity of (222) peak has the highest value. In addition, up to a certain point, the addition of boric acid results in slight increase in (222) peak intensity. By contrast, further use of the additive, significantly decreases the diffraction intensity (see Table 2).

As a matter of fact, H_3BO_3 acts as a flux material. With the use of small amounts of the additive, the crystallinity of synthesized phosphor is improved. This issue is related to the fact that small quantities of H_3BO_3 with a relatively lower melting point act as flux material and enhance the growth of yttria crystals [17]. In other words, it was found that the addition of small amounts of boric acid has

Table 2 Results obtained from the XRD spectra of A-H composites

Compound	Angle (2θ)	I	d (Å)
A	29.397	1497.4	3.035
B	29.161	1997.96	3.059
C	29.219	1072.38	3.053
D	29.233	667.71	3.052
E	27.417	1304.59	3.250
F	27.259	2288.71	3.268
G	27.204	1373	3.275
H	27.280	892.11	3.266

enlarged the distance of (222) plane from 3.035 to 3.059 Å (see Fig. 1b), implying the expansion of Yttria unit cell. But higher amounts of H_3BO_3 not only decrease the peak intensity, but also get constrict the inter-planar distance from 3.059 to 3.053 and 3.052 Å. This observation reveals that relatively larger amounts of H_3BO_3 suppress the growth of Y_2O_3 material. It seems that, the flux material provides efficient obstacles among the produced oxide nanoparticles.

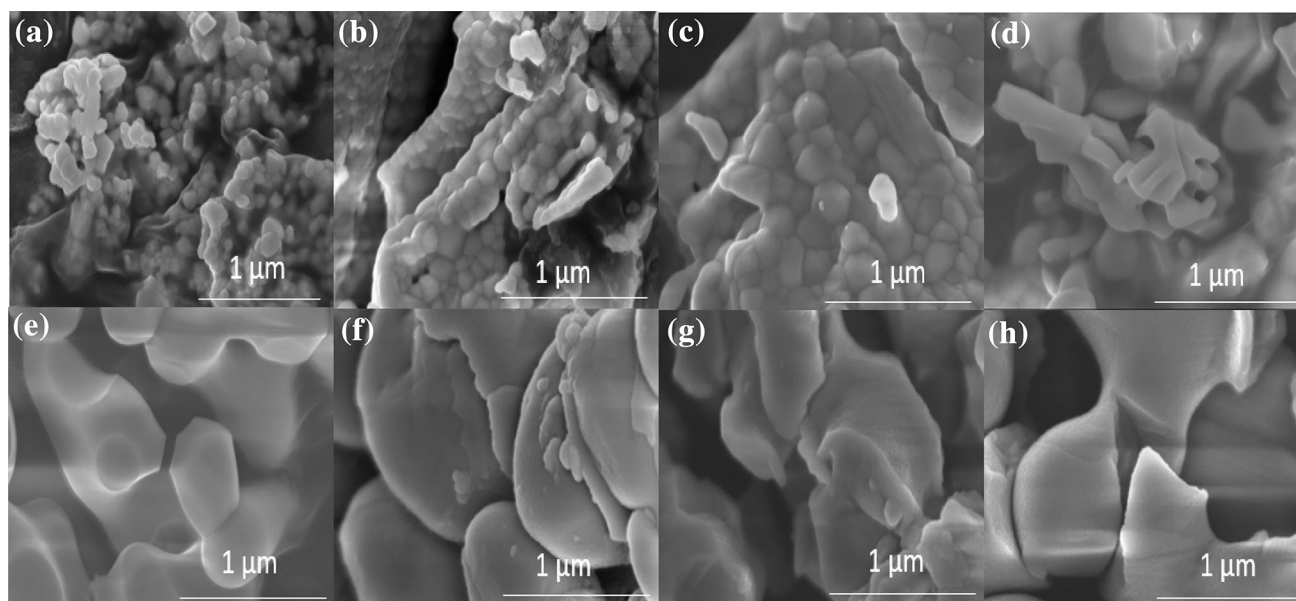
The study of XRD spectra of E–H compounds shows that the main diffraction peaks have occurred in different angles compared to those observed for A–D compounds. For instance, it is interestingly seen that through the addition of high magnitudes of H_3BO_3 , a relatively weak peak has emerged at approximately 27.4° . The evaluation of XRD spectra of E–H phosphors confirms that the synthesized materials are well crystallized with a hexagonal crystal structure (JCPDS No. 16-0277), consistent with

YBO_3 . The main diffractions are related to (002), (010), (102), (110), (104), (112), (200), (202), (114) planes, where (010) has the highest intensity. In other words, it was found that through consuming large amounts of H_3BO_3 , the formation of yttrium borate (YBO_3), with hexagonal structure space group $P63/mmc$ and lattice parameters of $a = 3.778$ and $c = 8.814$ Å, may be feasible.

Similar to what was explained for crystallite size estimation of phosphor A, the crystallite size of 75.7 nm can be calculated for phosphor E. Noteworthy, since the melting point of boric acid, 171°C , is much lower than the temperature of solid-state procedure, remarkable amounts of this flux material are subject to evaporation via solid-state procedure. Hence, slight increase in H_3BO_3 provides a situation to compensate the lost flux, improving the peak intensity of (010) (compare phosphors E and F). Also, the inter-planar distance of (010) plane enlarges from 3.250 to 3.268 Å, explaining the expansion of the H_3BO_3 crystal structure. Conversely, further addition of H_3BO_3 decreases the peak intensity, sensitively. This result means that the addition of relatively high amounts of boric acid decelerates the growth of the oxide materials. Clearly, the comparison of G, H phosphors shows that via the increase in H_3BO_3 , the (010) inter-planar distance decreases from 3.275 to 3.266 Å.

FESEM observations

Figure 2 shows the FESEM images of A–H compounds. Figure 2a shows that the employment of solid-state procedure results in the formation of nanoparticles. It can be easily found that the addition of H_3BO_3 results in the

**Fig. 2** FESEM images of A–H luminescent compounds

increase in particle size. In other words, the particle size of solid-state synthesized $\text{Y}_2\text{O}_3:\text{Eu}^{3+}$ phosphor is approximately 85 nm, while for compounds B, C and D, the particle size increased to 100, 120 and 200 nm, respectively. So, it is obvious that the presence of H_3BO_3 via solid-state procedure leads to severe grain growth. In addition, the surface area and the particle size of productions were characterized by BET equipment. The particle size of prepared compounds measured by the employed BET analyzer confirmed the observed particle sizes of FESEM images.

It is very interesting that when the added flux material is equal to the stoichiometric values, required for the formation of YBO_3 , the particle size and morphology change dramatically. As a case in point, it is seen that the particle sizes of phosphors A and F are about 100 nm and 1 μm , respectively. Henceforth, whenever the amount of boric acid exceeds the stoichiometric quantity, the particle size

decreases gradually. This issue is because H_3BO_3 material plays the role of obstacles, preventing grain growth.

PL analysis

Figure 3 shows the photoluminescence excitation and emission spectra of A-H compounds. The photoluminescence excitation of $\text{Y}_2\text{O}_3:\text{Eu}^{3+}$ phosphor is shown in Fig. 3a. Accordingly, there is a wide band from 200 to 300 nm that is due to the charge transfer (CT) from O^{2-} to Eu^{3+} ions with the levels of 2p and 4f, respectively [12]. Figure 3b shows the photoluminescence emission properties of $\text{Y}_2\text{O}_3:4\%\text{Eu}/\text{H}_3\text{BO}_3$ phosphors at the ambient temperature. The peaks are attributed to the trivalent Eu^{3+} ions with the forbidden transition of f–f, known as $^5\text{D}_0-^7\text{F}_J$ ($J = 0, 1, 2$). The weaker emissions which appear at about 587.8, 593.4 and 599.6 nm correspond to the $^5\text{D}_0-^7\text{F}_1$ transition. The $^5\text{D}_0-^7\text{F}_1$ magnetic dipole transition is

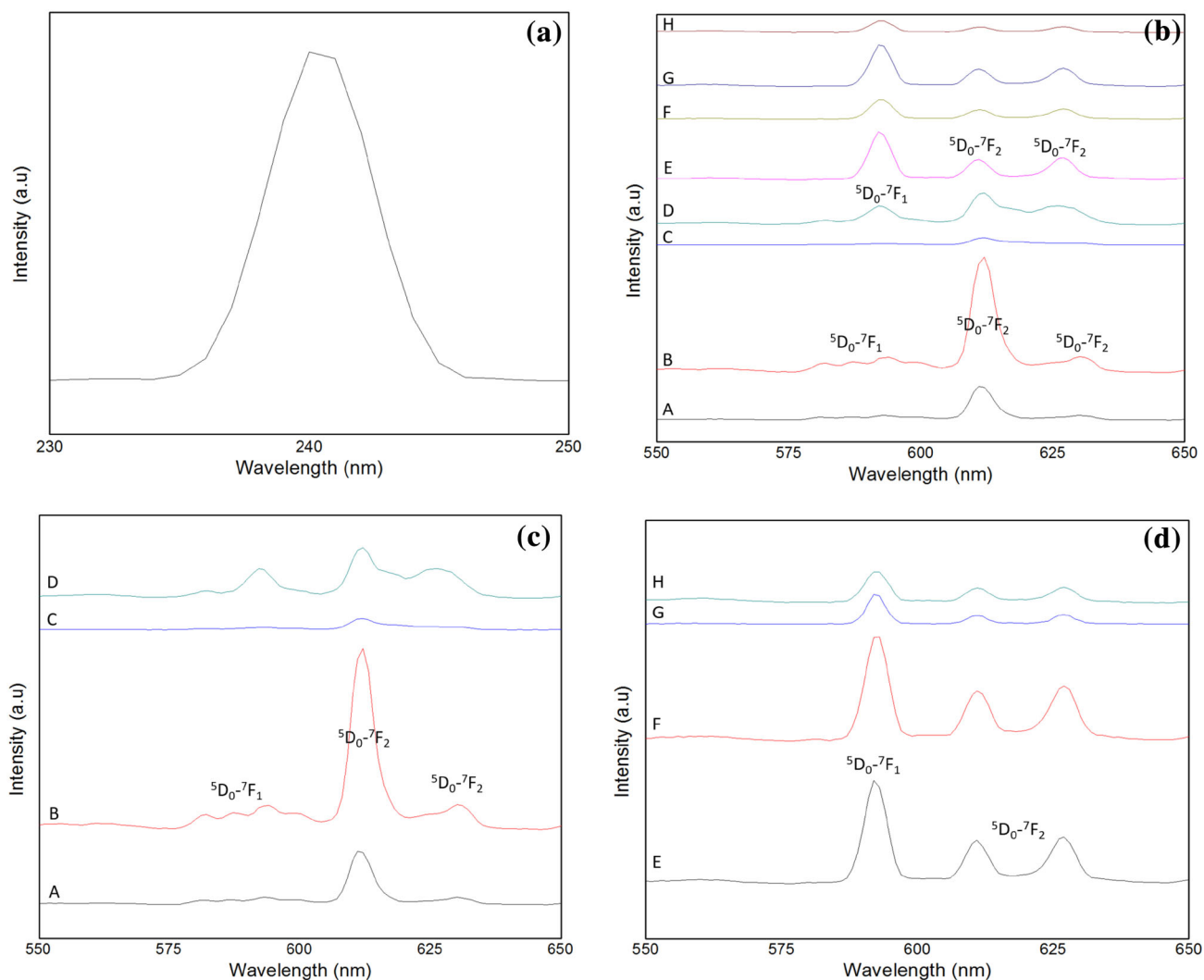
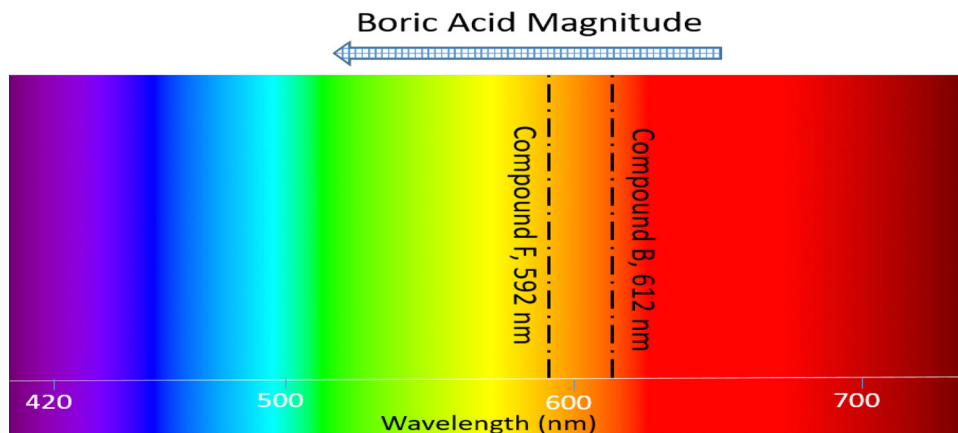


Fig. 3 Photoluminescence: **a** excitation of A, **b** emission of A-H, **c** emission of A-D and **d** emission of E-H compounds

Fig. 4 Wavelength spectrum of synthesized compounds



known as the parity allowed transition ($\Delta J = 1$), and its intensity usually remains independent of the host crystal. But the prominent emission band at approximate wavelength of 612 and 631.2 nm is due to the ${}^5D_0-{}^7F_2$ transition. The ${}^5D_0-{}^7F_2$ electric dipole transition ($\Delta J = 2$) is highly affected by the local environment around Eu^{3+} ions. So the emission intensity depends on the symmetry of the crystal field around the europium ions [18]. Figure 3c, which belongs to the emission behavior of A-D compounds, shows that the prominent ${}^5D_0-{}^7F_2$ peak has occurred at 612 nm [19]. Furthermore, it is seen that the addition of small amounts of boric acid to the rare earth-doped Y_2O_3 oxide (phosphor B) enhances the luminescence properties, efficiently. This issue, which is consistent well with the XRD spectra, reveals that use of boric acid has improved crystallinity of yttria host lattice. By contrast, it was found that higher quantities of the flux material result in the suppression of luminescence behavior that is very similar to the results reported by other researchers [20].

According to Fig. 3d, under the excitation wavelength of 240 nm, a strong band is seen at 592 nm which is related to the magnetic dipole transition of ${}^5D_0-{}^7F_1$ of Eu^{3+} ions [18]. YBO_3 host material has a hexagonal crystal structure in which Y^{3+} ions are surrounded by BO_3 groups. By doping of Eu element in YBO_3 oxide material, Eu ions are substituted into trivalent Y ions, providing a symmetry center and also a strong ${}^5D_0-{}^7F_1$ transition. In addition, two relatively weaker bands at the approximate wavelengths of 612 and 631 nm are related to the ${}^5D_0-{}^7F_2$ electric dipole transition. In other words, with the crystal change from cubic to hexagonal, the type of emission has been changed significantly. As per Judd–Ofelt theory [21], the intensity of transition between different levels depends upon the symmetry of the local environment of the Eu^{3+} activator. Meanwhile, the color purity of Eu^{3+} emission is characterized by $({}^5D_0-{}^7F_2)/({}^5D_0-{}^7F_1)$ ratio [22]. For YBO_3 , the C_i and C_1 sites are the well-known locations for the trivalent

Eu ions. For ${}^5D_0-{}^7F_1$ transition, the photoluminescence emission appears from both C_i and C_1 sites, while for ${}^5D_0-{}^7F_2$, only C_1 sites are considered since the C_i locations do not contribute to the emission characteristics [23]. As a matter of fact, the optical properties of phosphors depend on wide ranges of parameters. Zhenggui Wei et al. reported about the influence of particle size of $\text{YBO}_3:\text{Eu}$ phosphors on chromaticity characteristics [24].

It was found that the strongest and weakest intensities of PL spectra are related to F and H compounds, respectively. The relatively lower PL intensity of sample E compared to that of sample F may be attributed to the fact that H_3BO_3 has a boiling point of 300 °C and there is a huge loss of this material at the employed high-temperature solid-state procedure. So, it seems that the higher quantity of boric acid consumed in sample F compensates the loss of H_3BO_3 , providing more perfect crystal structure and stronger luminescence properties. Further increase in H_3BO_3 (G, H phosphors), providing some impurities in the compounds, suppresses the intensity of PL.

As an overall conclusion, the emission wavelength of $\text{Y}_2\text{O}_3:\text{Eu}^{3+}/\text{YBO}_3:\text{Eu}^{3+}$ -based phosphors is considered. The wavelength spectrum of compounds B and F is shown in Fig. 4.

It can be found that the use of boric acid results in change of emitted color from reddish (612 nm) to orangish (592 nm) for $\text{Y}_2\text{O}_3:\text{Eu}^{3+}$ -based compounds.

Conclusions

Nanoparticles of $(\text{Y}_{0.96}\text{Eu}_{0.04})_2\text{O}_3$ phosphor were synthesized through a facile solid-state method. It was found that using different amounts of boric acid not only changes the crystal structure of phosphors from cubic to hexagonal, but also affects the morphology and particle size of $\text{Y}_2\text{O}_3:\text{Eu}^{3+}$ phosphors, dramatically. Moreover, the PL emission wavelengths of obtained productions are influenced by the

addition of flux, effectively. Interestingly, it was found that the color of emission varies from reddish to orangish wavelengths by the use of boric acid.

Acknowledgements Hereby we acknowledge the finance support of Golpayegan University of Technology.

Open Access This article is distributed under the terms of the Creative Commons Attribution 4.0 International License (<http://creativecommons.org/licenses/by/4.0/>), which permits unrestricted use, distribution, and reproduction in any medium, provided you give appropriate credit to the original author(s) and the source, provide a link to the Creative Commons license, and indicate if changes were made.

References

- Dai, Q.L., Foley, M.E., Breshike, C.J., Lita, A., Strouse, G.F.: Ligand-passivated Eu:Y₂O₃ nanocrystals as a phosphor for white light emitting diodes. *J. Am. Chem. Soc.* **133**, 15475–15486 (2011)
- Qin, X.P., Zhou, G.H., Yang, H., Yang, Y., Zhang, J., Wang, S.W.: Synthesis and upconversion luminescence of monodispersed, submicron-sized Er³⁺:Y₂O₃ spherical phosphors. *J. Alloys. Compd.* **493**, 672–677 (2010)
- Wang, C.N., Li, Y., Zhang, W.P., Yin, M.: Effect of acidity on microstructure and spectroscopic properties of Y₂O₃:Eu³⁺ powders and ceramics. *Spectrochim. Acta A.* **75**, 8–13 (2010)
- Sharma, S.K.: Temperature dependent emission characteristics of monoclinic YBO₃: Eu³⁺/Tb³⁺ Phosphor. *J. Lumin.* **173**, 231–236 (2016)
- Kumar, Y., Pal, M., Herrera, M., Mathew, X.: Effect of Eu ion incorporation on the emission behavior of Y₂O₃ nanophosphors: a detailed study of structural and optical properties. *Opt. Mater.* **60**, 159–168 (2016)
- Gao, L., Wang, G., Zhu, H., Zhou, W., Ou, G.: Hydrothermal synthesis of Y₂O₃ coated Y₂O₃:Eu³⁺ nanotubes for enhanced photoluminescence properties. *Mater. Res. Bull.* **70**, 876–880 (2015)
- Mancic, L., Lojpur, V., Marinkovic, B.A., Dramicanin, M.D., Milosevic, O.: Hydrothermal synthesis of nanostructured Y₂O₃ and (Y_{0.75}Gd_{0.25})₂O₃ based phosphors. *Opt. Mater.* **35**, 1817–1823 (2013)
- Vazquez, R.M., Hernandez, M.G., Marure, A.L., Camacho, P.Y.L., Ramirez, A.D.J.M., Conde, H.I.B.: Sol–gel synthesis and antioxidant properties of yttrium oxide nanocrystallites incorporating P-123. *Mater.* **7**, 6768–6778 (2014)
- Ko, M.G., Park, J.C., Kim, D.K., Byeon, S.H.: Low-voltage cathodoluminescence property of Li-doped Gd_{2-x}Y_xO₃:Eu³⁺. *J. Lumin.* **104**, 215–221 (2003)
- Rafiaei, S.M., Kim, A., Shokouhimehr, M.: Enhanced luminescence properties of combustion synthesized Y₂O₃: Gd nanostructure. *Curr. Nanosci.* **12**, 244–249 (2016)
- Shokouhimehr, M., Rafiaei, S.M.: Combustion synthesized YVO₄:Eu³⁺ phosphors: effect of fuels on nanostructure and luminescence properties. *Ceram. Int.* **43**, 11469–11473 (2017)
- Kabira, M., Ghahari, M., Afarani, M.S.: Co-precipitation synthesis of nanoY₂O₃:Eu³⁺ with different morphologies and its photoluminescence properties. *Ceram. Int.* **40**, 10877–10885 (2014)
- Pang, Q., Shi, J., Liu, Y., Xing, D., Gong, M., Xu, N.: A novel approach for preparation of Y₂O₃:Eu³⁺ nanoparticles by microemulsion-microwave heating. *Mater. Sci. Eng., B* **103**, 57–61 (2003)
- Yu, H., Wang, H., Li, T., Che, R.: Preparation and luminescent properties of YBO₃: Eu nanofibers by electrospinning. *Appl. Phys. A* **108**, 223–227 (2012)
- Rafiaei, S.M.: Effect of flux compounds on the luminescence properties of Eu³⁺ doped YBO₃ phosphors. *Mater. Sci. Pol.* **34**, 780–785 (2016)
- Jung, D.S., Hong, S.K., Lee, H.J., Kang, Y.C.: Gd₂O₃: Eu phosphor particles prepared from spray solution containing boric acid flux and polymeric precursor by spray pyrolysis. *Opt. Mater.* **28**, 530–535 (2006)
- Koo, H.Y., Ju, S.H., Hong, S.K., Jung, D.S., Kang, Y.C., Jung, K.Y.: Effect of boric acid flux and drying control chemical additive on the characteristics of Y₂O₃: Eu phosphor particles prepared by spray pyrolysis. *Jpn. J. Appl. Phys.* **45**, 9083–9087 (2006)
- Jadhav, A.P., Pawar, A.U., Pal, U., Kang, Y.S.: Red emitting Y₂O₃:Eu³⁺ nanophosphors with > 80% down conversion efficiency. *J. Mater. Chem. C* **2**, 496–500 (2014)
- Rafiaei, S.M., Kim, A., Shokouhimehr, M.: Effect of Solvent on Nanostructure and Luminescence properties of combustion synthesized Eu³⁺ Doped Ytria. *Nanosci. Nanotech. Lett.* **6**, 692–696 (2014)
- Jung, K.Y., Lee, C.H., Kang, Y.C.: Effect of surface area and crystallite size on luminescent intensity of Y₂O₃: Eu phosphor prepared by spray pyrolysis. *Mater. Lett.* **59**, 2451–2456 (2005)
- Nair, R.G., Nigam, S., Vishwanadh, B., Sudarsan, V., Vatsa, R.K., Majumder, C., Jain, V.K.: Size induced modification of boron structural unit in YBO₃: systematic investigation by experimental and theoretical methods. *RSC. Adv.* **6**, 64065–64071 (2016)
- Yano, K., Takeshita, S., Iso, Y., Isobe, T.: Combinatorial optimization of the atomic compositions for green-emitting YBO₃:Ce³⁺, Tb³⁺ + and red-emitting YBO₃:Ce³⁺, Tb³⁺ +, Eu³⁺ + phosphors using a microplate reader. *RSC. Adv.* **7**, 17586–17592 (2017)
- Chen, L., Deng, X., Xue, S., Bahader, A., Zhao, E., Mua, Y., Tian, H., Lu, S., Yu, K., Jiang, Y., Chen, S., Tao, Y., Zhang, W.: The energy transfer in the Sb³⁺ and Eu³⁺ co-activated YBO₃ phosphor and their white luminescence for deep ultraviolet LEDs application. *J. Lumin.* **149**, 144–149 (2014)
- Wei, Z., Sun, L., Yin, C.J., Jiang, X., Yan, C.: Size-dependent chromaticity in YBO₃: Eu nanocrystals: correlation with microstructure and site symmetry. *J. Phys. Chem. B* **106**, 10610–10617 (2002)

Publisher's Note

Springer Nature remains neutral with regard to jurisdictional claims in published maps and institutional affiliations.

